

Reports

Airglow and Star Photographs in the Daytime from a Rocket

Abstract. Photographs of the constellation Cygnus taken in the daytime from altitudes above 100 kilometers indicate that the day sky brightness in the wavelength region from 3600 to 7000 angstroms is only slightly brighter than the night sky viewed from the ground. No diffuse cloud of particles was apparent in the vicinity of the rocket payload, but discrete particles must be considered in the design of instruments for rockets and satellites. The resultant data and reports of star sightings from manned spacecraft indicate similar optical environments for both types of vehicles, that is, discrete particles and relatively low levels of background brightness, only slightly brighter than the night sky as an upper limit.

Daytime photographs of the constellation Cygnus have been obtained with a Nikon camera ($f/1.4$; 50-mm effective focal length) and extremely fast panchromatic film (Eastman Kodak SO-166, now marketed as Kodak 2485). The camera lens was protected from illumination by the sun and earth by the proper selection of the orientation of the rocket body and the use of a large shade, with multiple conic sections, carefully designed so that a minimum of three reflections was necessary in order that stray light strike the lens. Because of improper pointing of the rocket, only two reflections occurred. The sharp edge of a field-defining aperture was thus illuminated by secondary reflection of sunlight, and its out-of-focus image is seen in Fig. 1.

Twenty photographs similar to the figure were used to determine (i) the solution of the roll aspect for the initial firing of a solar-pointing control rocket (Aerobee 150; NASA 4.201 NT) and (ii) the optical environment at sounding rocket altitudes, especially day glow and scattered light from particulate matter in the vicinity of the payload. The rocket was launched at 1500 M.S.T. on 10 December 1967 from White Sands Missile Range, New Mexico. Usable photographs were obtained at altitudes from 70 to 160 km. During the flight the angle between the sun

and the optical axis of the camera varied from 95° to 70° . Scattered light from the field-defining aperture was detected. No significant amount of the observed background brightness of the sky can be attributed to light scattered within the instrument.

The photographs have been interpreted photometrically by calibration against a tungsten low-brightness source

at an effective temperature of 2360°K , a calibrated gray scale, and 1000-watt tungsten source calibrated by the National Bureau of Standards. The relative spectral sensitivity of the camera system was determined by combining film data (1) with our transmission measurements of the camera lens.

The relative spectral response of the system is a smooth function with values of approximately 0.05 at 3600 Å; 1.0 at 4300 Å (by definition); 0.3 from 5000 to 6800 Å; and 0.05 at 7000 Å. Photometric calibration, based on the low-brightness source at a temperature of 2360°K and the NBS lamp, was internally consistent within a range of about ± 25 percent. Comparison was made to ground-based photographs of the constellation Orion taken from White Sands Missile Range at about 2200 M.S.T. on 29 November 1967, a very clear night. Using data on airglow from Allen (2) and values of the stellar background brightness from Roach (3), we derived the photometric response of the system from these photographs.

Exposures (each 4 seconds long) were made every 10 seconds of flight from 54 to 404 seconds after launch except for a 24-second exposure beginning at 154 seconds (135 to 150 km) and a 34-second exposure beginning at 214 seconds (160 to 156 km). Usefully exposed photographs were obtained from 94 to 324 seconds after

Table 1. Background surface brightness of the day sky.

Space vehicle	Brightness*	Observational technique†	Magnitude‡ limit to eye (m_v)
Aerobee 150	1×10^{-12} (total); 5×10^{-13} (upper limit due to cloud)	Photography	To limit (inferred)
Gemini V	5×10^{-9} (observed)	Eye (8)	Fainter than +2 (observed)
Gemini VI	10^{-11} – 10^{-12} (observed upper limit)	Eye (9)	Fainter than +4.5 (observed to limit of dark adaptation of observer)
Orbiting Geophysical Observatory OGO III	5×10^{-13} (observed upper limit)	Image dissector (10)	To limit (inferred)
Gemini	3×10^{-11} (calculated minimum)	Calculation (11)	+4.5 (calculated)
Apollo	1×10^{-13} (calculated minimum)	Calculation (11)	To limit
	<i>Mean brightness of night sky from ground</i>		
	1.5×10^{-18}	Summary of many observations (2)	To limit§

* In units of fraction of mean solar brightness, which is 2×10^8 stilb. † No experiment has yet detected a surface brightness which can be attributed to a spacecraft "cloud." ‡ Ultimate limit of the eye under dark adaptation is between visual magnitude +6 and +7. § The ultimate limit of ground-based instruments is fainter than +22 m_v .

launch, for an altitude range from about 70 km up to a peak altitude of 160 km and down to about 95 km. Peak altitude was attained at about 215 seconds after launch. The photograph at 94 seconds (65 to 75 km) had a relative diffuse brightness of 250, and the photograph at 104 seconds (86 to 96 km) had a relative brightness of 80; all other photographs had a relative brightness of 30 ± 5 , independent of altitude. The relative diffuse brightness in the vicinity of Orion observed from the ground was about 8 ± 2 . Limiting stellar magnitude in flight was $+8 m_v$ (visual magnitude) or slightly fainter. This was consistent with the limit (fainter than $+11 m_v$) attained from the ground with the same camera system.

The difference in the limiting magnitude for the two observations is attributable to the fact that the instantaneous exposure in flight was 0.4 second or shorter (Fig. 1) due to motion of the payload. The high degree of brightness in the first two exposures is consistent with the expected levels of Rayleigh scattering from the earth's atmosphere at the lower altitudes. Since Rayleigh scattering varies directly with

number density at low light levels, the background brightness above about 100 km cannot be caused by such scattering because it is independent of altitude. It must therefore be attributed to day airglow or scattering in the vicinity of the payload or both.

In order to determine the source of the diffuse brightness, it was necessary to correct the data for stellar background, zenith angle, spectral response of the camera system, and spectral characteristics of the various sources of radiation. The approximate zenith angle for the optical axis of the camera was 60° for Orion and 12° for Cygnus. The spectrum of the night airglow was assumed to be the same as that presented by Allen (2). The visual component of the airglow has a surface brightness of about 210 S10V units (one S10V unit is the equivalent surface brightness produced by one 10th- m_v star per square degree). The stellar background was assumed to be spectrally independent of variation in wavelength. The stellar background brightness was assumed to be 150 S10V units in the Orion region and 350 S10V units in the region of Cygnus (3). Incidentally, the North American Nebula was

identified in several of the photographs taken when the motion of the payload was small.

Because the spectral distribution of the daytime sky brightness is not known and the camera system has a very wide response, there are several ways in which the actual spectral distribution might be deduced. The simplest way is to assume the relative ratio between the day and night photographs, which leads to a brightness ratio of

$$\frac{\text{Day (Cygnus)}}{\text{Night (Orion)}} = 4 \pm 1$$

A second method would be to assume the same spectral distribution as that of the night airglow and to correct for the known stellar background. In this case the brightness ratio is

$$\frac{\text{"Day glow"}}{\text{Night glow}} = 9 \pm 6$$

The last method is to assume that all the brightness of the day sky not due to stars is caused by radiation at 3914 Å. Our observation indicates a day glow brightness of 8 ± 4 kr (photometry at 2360°K) or 7 ± 4 kr (photography of Orion). (One kilorayleigh of radiation at 3914 Å is equivalent to a surface brightness of 0.41×10^{-3} erg sec $^{-1}$ sr $^{-1}$).

Wallace and McElroy (4) indicate that the effective radiation at 3914 Å is 3.3 kr [that is, 2 kr (3914 Å) + 1.75 kr (5577 Å) + 2.75 kr (6300 Å) = 3.3 kr (3914 Å as observed by our camera system)]. This level of sky brightness accounts for approximately one-half of the noncelestial day sky brightness that we detected. The nature of the day glow continuum is not known from any observation, but, with the wide spectral range of the camera system, the remaining one-half of the radiation could easily be attributed to the day glow continuum, without any implied reference to a debris "cloud" in the vicinity of the payload. The result of this observation from the Aerobee rocket is compared to the optical environment viewed from manned and unmanned spacecraft in Table 1.

During the flight about 25 small (dust?) particles illuminated by direct sunlight were photographed as they passed through the field of view of the camera. Measurement of the size of the out-of-focus image indicated that 19 of the particles were within 3 m of the lens and that ten of these

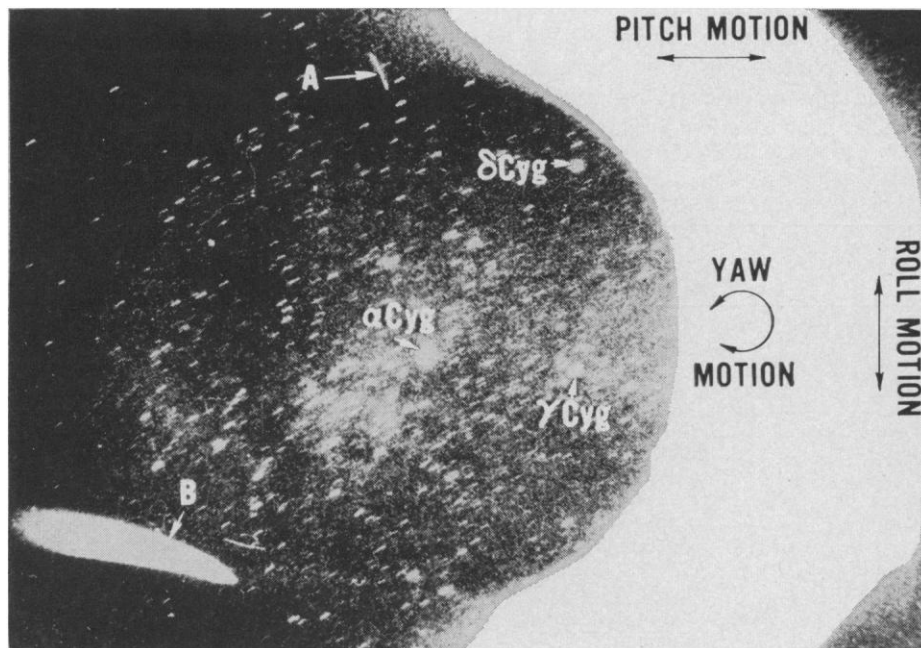


Fig. 1. A 4-second exposure of the constellation Cygnus taken in the daytime. The altitude was 154 km and the configuration of the payload is labeled. Two particles are seen in the photograph: *A*, at some distance from the camera; *B*, from 50 to 75 cm from the camera. The large bright semicircle to the right is the out-of-focus image of a field-defining diaphragm 9 cm from the lens. The absence of instrumental scattered light can be noted by the dark corners, which receive no light from outside the camera. The positive roll axis is directed toward the sun. The angle between the optical axis and the sun is 84° . Because of motion of the payload, the effective exposure time for stars is approximately 0.4 second at the maximum. The faintest stars photographed are about $+8 m_v$.

originated within the camera shade. (They were in direct sunlight within 10 cm of the camera lens.) The remainder of the particles were of small angular dimension at relatively infinite distances from the camera. It is extremely likely that such particles are present on any Aerobee flight and probably cannot be eliminated completely even with extreme precautions. It may be that such particles could account for the stray light signals reported by Wallace and McElroy (4) which, however, did not seriously detract from their results. Similar particles have been observed in coronagraph experiments on Aerobee rockets at small angles from the sun (5). Discrete particles have been observed and photographed from manned spacecraft (6).

The most significant conclusion that may be drawn from the daytime rocket photographs is that the day sky brightness in the photographic spectral region over the altitudes covered is only slightly brighter than that of the night sky. Our data for day glow brightnesses are generally consistent with the values observed photoelectrically by Wallace and McElroy (4). Such observations of the stellar aspect (low brightness) can be made in the daytime as well as at night (7) but extreme precaution should be used in designing equipment for daytime low-brightness observations because sunlight is scattered from discrete particulate matter nearby and from rocket and spacecraft payloads.

D. C. EVANS

L. DUNKELMAN

Goddard Space Flight Center,
National Aeronautics and Space
Administration, Greenbelt, Maryland

References and Notes

1. Kodak 2485 High-Speed Recording Film Data Release (Eastman Kodak Company, Rochester, N.Y., 1967).
2. C. W. Allen, *Astrophysical Quantities* (Athlone Press, Univ. of London; Oxford Univ. Press, New York, ed. 2, 1963).
3. F. E. Roach, *Space Sci. Rev.* 3, 512 (1964); personal communication.
4. L. Wallace and M. B. McElroy, *Planet. Space Sci.* 14, 677 (1966).
5. R. Tousey, M. J. Koomen, R. E. McCullough, R. T. Seal, *NASA (Nat. Aeronaut. Space Admin.) SP-135* (1955).
6. J. A. O'Keefe, L. Dunkelman, S. D. Soules, W. F. Huch, P. D. Lowman, Jr., *NASA (Nat. Aeronaut. Space Admin.) SP-45* (1963), p. 342.
7. J. P. Hennes and L. Dunkelman, *J. Geophys. Res.* 71, 755 (1966).
8. E. P. Ney and W. F. Huch, *Science* 153, 297 (1966).
9. D. C. Evans and L. Dunkelman, *Astron. J.* 72, 795 (abstract) (1967).
10. C. Wolff, *Science* 158, 1045 (1967).
11. G. Newkirk, Jr., *Planet. Space Sci.* 15, 1267 (1967).

9 April 1969

20 JUNE 1969

Convergence and Strain Waves Caused by a Submerged Turbulent Disturbance in Stratified Fluids

Abstract. Short bursts of submerged turbulent mixing in stratified water (everywhere denser below than above) is shown to cause waves of surface convergence, divergence, and strain. Quantitative data are given for four experiments.

The phenomenon of "wake-collapse," caused by the passage of a submerged self-propelled body in a stratified fluid was initially reported in 1963 (1). The submerged turbulently mixed wake first expands due to turbulent momentum. It then reaches a vertical maximum. This is followed by a vertical contraction (collapse) accompanied by continued spreading horizontally. The collapse phase is an efficient generator of internal waves in the stratified fluid (1, 2). The phase of wake collapse for the time between the initiation of submerged turbulent mixing and the time of maximum vertical expansion of the wake, before it starts to collapse, has been considered earlier (1, 3, 4).

The present experiments yield data

on the approximate maximum convergence and strain that reach the surface and travel outward from a point above a submerged turbulent disturbance. The apparatus consisted of a transparent cell 2.5 cm thick, 7.3 cm deep, and 30 cm long with internal wave dampers at the ends. The cell was filled with water between top and bottom copper strips, and stratification was introduced by cooling the bottom and heating the top with thermoelectric devices. A brief and repeatable turbulent disturbance, centered and 4.5 cm below the surface, was used to simulate the passage of a self-propelled body perpendicular to a narrow "slice" of stratified fluid (3, 4). Thermistors at positions along and near the upper surface measured wavelike convergence and divergence flows as

Table 1. Vertical profiles of temperature and Väisälä-Brunt period, specifying four different water stratifications used for the experiments z , depth; Θ , temperature; T , period; i , imaginary.

z (cm)	Experiment a		Experiment b		Experiment c		Experiment d	
	Θ (°C)	T (sec/cy)	Θ (°C)	T (sec/cy)	Θ (°C)	T (sec/cy)	Θ (°C)	T (sec/cy)
0	50.0	2.9	29.5	6.3	22.2	15.0	17.2	i
1	40.0	3.7	25.8	6.7	21.1	15.0	17.6	i
2	32.5	4.4	22.9	7.5	20.1	15.0	17.7	i
3	27.3	5.4	20.5	8.9	19.3	15.0	17.4	19.0
4	22.4	6.3	17.8	9.7	18.5	15.0	16.7	14.0
4.5	19.5	6.8	16.6	9.8	18.1	15.0	15.9	13.1
5	18.5	7.4	15.5	9.9	17.7	15.0	15.2	12.3
6	14.3	8.2	12.5	10.0	16.7	15.0	13.2	11.7
7	6.5	8.8	9.3	10.2	15.7	15.0	10.6	11.7

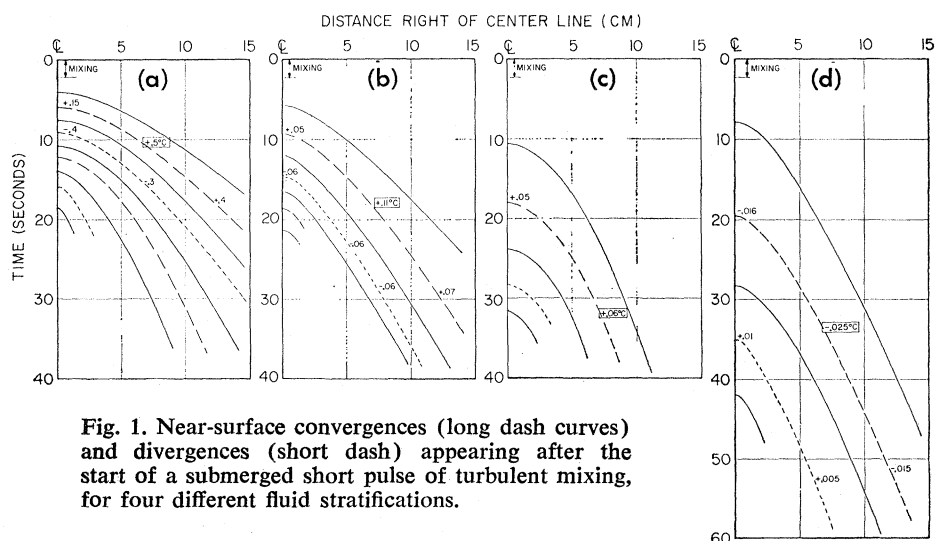


Fig. 1. Near-surface convergences (long dash curves) and divergences (short dash) appearing after the start of a submerged short pulse of turbulent mixing, for four different fluid stratifications.